Front. Phys. 12(5), 127101 (2017)
DOI 10.1007/s11467-016-0625-y

RESEARCH ARTICLE

Superfluid response in heavy fermion superconductors

Yin Zhong[1,*], Lan Zhang[1], Can Shao, Hong-Gang Luo[1,2,†]

[1] *Center for Interdisciplinary Studies & Key Laboratory for Magnetism and Magnetic Materials of the MoE, Lanzhou University, Lanzhou 730000, China*
[2] *Beijing Computational Science Research Center, Beijing 100084, China*
*Corresponding authors. E-mail: * zhongy05@hotmail.com; † luohg@lzu.edu.cn*
Received July 20, 2016; accepted August 24, 2016

Motivated by a recent London penetration depth measurement [H. Kim, et al., *Phys. Rev. Lett.* 114, 027003 (2015)] and novel composite pairing scenario [O. Erten, R. Flint, and P. Coleman, *Phys. Rev. Lett.* 114, 027002 (2015)] of the Yb-doped heavy fermion superconductor $CeCoIn_5$, we revisit the issue of superfluid response in the microscopic heavy fermion lattice model. However, from the literature, an explicit expression for the superfluid response function in heavy fermion superconductors is rare. In this paper, we investigate the superfluid density response function in the celebrated Kondo–Heisenberg model. To be specific, we derive the corresponding formalism from an effective fermionic large-N mean-field pairing Hamiltonian whose pairing interaction is assumed to originate from the effective local antiferromagnetic exchange interaction. Interestingly, we find that the physically correct, temperature-dependent superfluid density formula can only be obtained if the external electromagnetic field is directly coupled to the heavy fermion quasi-particle rather than the bare conduction electron or local moment. Such a unique feature emphasizes the key role of the Kondo-screening-renormalized heavy quasi-particle for low-temperature/energy thermodynamics and transport behaviors. As an important application, the theoretical result is compared to an experimental measurement in heavy fermion superconductors $CeCoIn_5$ and Yb-doped $Ce_{1-x}Yb_xCoIn_5$ with fairly good agreement and the transition of the pairing symmetry in the latter material is explained as a simple doping effect. In addition, the requisite formalism for the commonly encountered nonmagnetic impurity and non-local electrodynamic effect are developed. Inspired by the success in explaining classic 115-series heavy fermion superconductors, we expect the present theory will be applied to understand other heavy fermion superconductors such as $CeCu_2Si_2$ and more generic multi-band superconductors.

Keywords heavy fermion superconductor, Kondo lattice system, superfluid density

PACS numbers 71.10.Hf, 71.27.+a

1 Introduction

Superfluid density, or London penetration depth measurement, is a fundamental experimental tool to detect low-temperature superconducting quasi-particle excitation in the highly entangled unconventional pairing ground-state [1–3]. The low-temperature behavior of such a quantity has provided invaluable information about the pairing symmetry for high-T_c cuprate, iron pnictide, and heavy fermion superconductors [4–13].

In the field of heavy fermion compounds, the power-law temperature dependence of superfluid density has been widely observed in the classic quasi-two-dimensional heavy fermion superconductor $CeCoIn_5$, with a remarkably high $T_c = 2.3$ K [7–12, 14]; although its detailed power-law behavior is still controversial due to proximity to possible magnetic quantum critical points [7–11]. By combining thermodynamic and transport measurements, such as heat capacity [15, 16], thermal conductivity [15, 17], dc magnetization [18], NMR [19], tunneling spectrum [20], and the observation of a characteristic (π, π, π) spin resonance mode and quasi-particle interference signal [21–24], $CeCoIn_5$ is now believed to be a nodal-$d_{x^2-y^2}$-wave superconductor, which has remarkable similarity to the well-known high-T_c cuprates.

Recently, London penetration depth measurements of Yb-doped $CeCoIn_5$, i.e., $Ce_{1-x}Yb_xCoIn_5$, have been per-

*arXiv: 1511.04167.

formed and, unexpectedly, the power-law behavior is gradually replaced with a fully gapped exponential behavior for increasing Yb-doping [13]. (However, a recent thermal conductivity measurement implies the nodal d-wave is robust and no pairing symmetry transition exists [25].) Such a surprising experimental finding is explained to be a change of pairing symmetry and even inspires an exotic local pairing scenario involving a composite molecular superfluid and Lifshitz transition of nodal Fermi surface [26].

However, when we try to understand the superfluid response in those heavy fermion superconductors from a theoretical standpoint, an explicit expression of the superfluid response function in the literature, particularly for the microscopic model Hamiltonian, is rare despite widespread and intensive experimental exploration. However, some phenomenological Fermi liquid-based arguments and superfluid density formulae of composite pairing do exist [27, 28]. In the present study, we investigate the superfluid density response function in the celebrated microscopic Kondo–Heisenberg model [29]. Specifically, we give a detailed derivation of the corresponding formalism from an effective fermionic large-N mean-field pairing Hamiltonian [30, 31], whose pairing interaction is assumed to originate from the effective local antiferromagnetic exchange interaction [32]. However, more conventional antiferromagnetic spin-fluctuation-exchange and resonance-valence-bond (RVB) theories give rise to the identical effective pairing Hamiltonian [29, 30, 33–36].

We find that the physically correct superfluid density formula can be obtained without any unsatisfactory breakdown only if the external electromagnetic field is assumed to directly couple to the heavy fermion quasiparticle rather than the bare conduction electron or local moment, see Fig. 1. Generally, this is the underlying feature when considering low-temperature/energy thermodynamics and transport; the physical fermionic excitation should be the (composite) heavy fermion quasiparticle [37], which results from nontrivial renormalization of collective Kondo screening effect. For superfluid density response considered in the present work to match the temperature/doping evolution of the superconducting heavy quasi-particle in the superfluid density formula, characteristic quantities, such as effective velocity and mass, have to describe the heavy quasiparticle, whose pairing drives the superconducting instability. These findings are presented below and contribute to the active field of heavy fermion systems.

As a crucial application of the derived superfluid response formula, we revisit undoped $CeCoIn_5$ and Yb-doped $Ce_{1-x}Yb_xCoIn_5$. For the former, there is good agreement between theory and experiment, confirming the present theoretical formalism that underlies the dominating heavy fermion excitations. Furthermore, when applied to the latter, we successfully explain the doping evolution of pairing symmetry in $Ce_{1-x}Yb_xCoIn_5$ as a simple doping effect by investigating its pairing strength. The calculated temperature-dependent superfluid density in both nodal d-wave and nodeless s-wave states is consistent with available measurements [13], which is a nontrivial confirmation of our theory. In addition, we have derived related formulas for general nonmagnetic impurities and non-local electrodynamic effects, which may be useful in realistic applications, e.g., La- and Nd-substituted $CeCoIn_5$ [13].

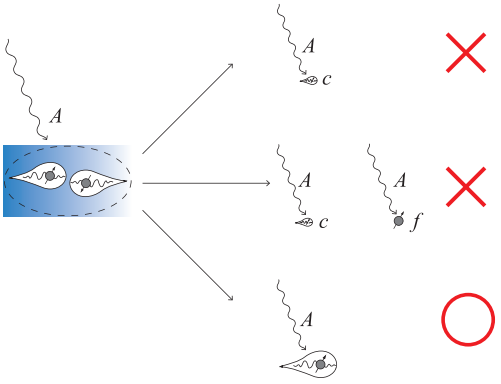

Fig. 1 The external electromagnetic field, $\boldsymbol{A}$, may couple to conduction electron (c-electron), auxiliary fermion (f-electron), and, more directly, the heavy fermion quasiparticle (large tadpole). Only the heavy fermion quasiparticle coupling is found to be responsible for realistic superfluid response in heavy fermion superconductors.

Having succeeded in explaining prototypical 115-series heavy fermion superconductors, we believe that the proposed formalism for superfluid response can be applied to understand other heavy fermion superconductors, such as the prototypical compound $CeCu_2Si_2$ and $PrOs_4Sb_{12}$ with possible time-reversal-symmetry breaking [38, 39], if proper modification and extensions are included. More generally, it is expected that our theory may also be useful for other multi-band superconductors, i.e., iron pnictide and $LaOs_4Sb_{12}$ [6, 40].

The remainder of this paper is organized as follows. In Section 2, the Kondo–Heisenberg model is introduced and its mean-field normal-state Hamiltonian is derived. In Section 3, the pairing interaction is discussed and the corresponding pairing Hamiltonian is derived. In Section 4, three different superfluid density formulas are derived and analyzed. We focus on the application of our theory to the heavy fermion superconductor $CeCoIn_5$ and its doped compound $Ce_{1-x}Yb_xCoIn_5$ in Section 5. In Section 6, both the impurity effect and non-local effect are discussed. Finally, Section 7 is devoted to a brief discussion and conclusion.

2 The Kondo–Heisenberg model and its normal-state Hamiltonian

The standard definition of the Kondo–Heisenberg model reads [29, 41]

$$H = \sum_{k\sigma} \varepsilon_k c^\dagger_{k\sigma} c_{k\sigma} + J_K \sum_i S^c_i \cdot S^f_i + J_H \sum_{\langle i,j\rangle} S^f_i \cdot S^f_j$$

For simplicity, the system is located on a regular square lattice and the resulting conduction electron band is $\varepsilon_k = -2t(\cos k_x + \cos k_y) + 4t' \cos k_x \cos k_y - \mu$ with chemical potential, μ. Extension to other lattices, such as triangular or honeycomb lattices, is straightforward [42, 43]. Next, we use fermionic representation to rewrite the degree of freedom of f-electron local spins as $S^f_i = \frac{1}{2}\sum_{\sigma\sigma'} f^\dagger_{i\sigma}\tau_{\sigma\sigma'} f_{i\sigma'}$, where τ is the standard Pauli matrices. If magnetism and Kondo screening are required to treat on the same footing, the supersymmetric representation of local spins is helpful and it is of interest to see whether this novel method can be applied to heavy fermion superconductivity [44]. Moreover, to exclude nonphysical charge fluctuations of the auxiliary fermion, f_σ, it is crucial to enforce the local constraint $\sum_\sigma f^\dagger_{i\sigma} f_{i\sigma} = 1$ at each site.

Physically, this model describes two competing tendencies. The first is Kondo screening, which leads to the formation of a collective spin-singlet state among local moments and conduction electrons. The second is the short-range antiferromagnetic fluctuations introduced by the Heisenberg interaction between local moments. The observed complicated phenomena in diverse heavy electron systems are believed to be captured by these two active factors. To obtain qualitatively correct information in the paramagnetic heavy fermion liquid state, the fermionic large-N or slave-boson mean-field theory is widely utilized [45, 46]. Here, we use the former to obtain an effective mean-field Hamiltonian.

2.1 Mean-field model in the paramagnetic state

After performing the standard large-N mean-field approximation [35, 41], we obtain the following Hamiltonian

$$H = \sum_{k\sigma} \Big[\varepsilon_k c^\dagger_{k\sigma} c_{k\sigma} + \chi_k f^\dagger_{k\sigma} f_{k\sigma} + \frac{J_K V}{2}(c^\dagger_{k\sigma} f_{k\sigma} + f^\dagger_{k\sigma} c_{k\sigma}) \Big] + E_0. \quad (1)$$

Here, the Kondo screening effect is encoded with an effective hybridization between conduction electron and local spins via $V = -\sum_\sigma \langle c^\dagger_{i\sigma} f_{i\sigma}\rangle$. Meanwhile, local spins acquire dissipation $\chi_k = J_H \chi \eta_k + \lambda$ with $\eta_k = \cos k_x + \cos k_y$ due to the formation of nearest-neighbor valence-bond order $\chi = \sum_\sigma \langle f^\dagger_{i\sigma} f_{j\sigma}\rangle$. Intuitively, such valence-bond order reflects the quantum dynamics of disordered local spins, which competes with magnetic long-range order. In addition, the Lagrangian multiplier, λ, is introduced to impose the local constraint on average and a constant energy shift, $E_0 = N_s(J_K V^2/2 + J_H \chi^2 - \lambda)$, where the number of lattice sites, N_s, is included.

Using the following quasi-particle transformation relation

$$\begin{aligned} c_{k\sigma} &= \alpha_k A_{k\sigma} - \beta_k B_{k\sigma} \\ f_{k\sigma} &= \beta_k A_{k\sigma} + \alpha_k B_{k\sigma}, \end{aligned} \quad (2)$$

where $\alpha^2_k = \frac{1}{2}(1 + \frac{\varepsilon_k - \chi_k}{E_{0k}})$, $\beta^2_k = \frac{1}{2}(1 - \frac{\varepsilon_k - \chi_k}{E_{0k}})$, $\alpha_k\beta_k = \frac{J_K V}{2E_{0k}}$, and $E_{0k} = \sqrt{(\varepsilon_k - \chi_k)^2 + (J_K V)^2}$. The original Hamiltonian, Eq. (1), is transformed into a diagonalized Hamiltonian

$$H = \sum_{k\sigma} (E^+_k A^\dagger_{k\sigma} A_{k\sigma} + E^-_k B^\dagger_{k\sigma} B_{k\sigma}) + E_0, \quad (3)$$

where $E^\pm_k = \frac{1}{2}(\varepsilon_k + \chi_k \pm E_{0k})$ is the quasi-particle energy for quasi-particles $A_{k\sigma}$ and $B_{k\sigma}$, respectively.

3 Pairing interaction in the Kondo–Heisenberg model

We are mainly interested in the superfluid response in the corresponding superconducting pairing phase; therefore, a proper superconducting model is required to perform any realistic and sensible calculation.

It has long been proposed that the introduced Heisenberg interaction can mediate spin-singlet pairing between conduction electrons via the pairing of auxiliary fermions in the present Kondo–Heisenberg model [24, 29, 30, 47]. Microscopically, the underlying mechanism of auxiliary fermion pairing can be attributed to the celebrated RVB state or, alternatively, the spin-fluctuation-exchange theory [33–35, 48]. However, to date, there is still no consensus on the mechanism of such an unconventional pairing and we must reconsider this issue with a more phenomenological approach [37].

Theoretically, in both RVB and spin-fluctuation-exchange theory, the superconducting pairing is induced by a particular effective antiferromagnetic interaction. The main difference is that the former emphasizes local real-space correlations while the latter is focused on dynamic exchange of energy/momentum, i.e., the collective antiferromagnetic fluctuations. In practice, since the observed pairing structure in heavy fermion superconductors has a strong momentum-dependent behavior, one may expect that the driving force of pairing is the space-dependent part of the effective pairing interaction

rather than its time/energy part. In other words, we may imagine a real-space pairing interaction and, if we take the magnetic (fluctuation) nature of interaction into account, we will arrive at the following phenomenological local magnetic exchange interaction [32]

$$H_{int} = \sum_{ij} J_{ij} \boldsymbol{S}_i^f \cdot \boldsymbol{S}_j^f.$$

The spin density operator denotes the spin degree of freedom of the local f-electron, which should result from the existing RKKY interaction. Furthermore, if only nearest-neighbor coupling is involved, this term naturally evolves into the Heisenberg term in the Kondo–Heisenberg model. That is to say that the Kondo–Heisenberg model itself has already included the basic element of superconducting pairing.

Now, we can write the Heisenberg interaction term into its momentum-space version [37]

$$H_H = \frac{1}{2} \sum_q J_q \boldsymbol{S}_q^f \cdot \boldsymbol{S}_{-q}^f,$$

where $J_q = 2J_H(\cos q_x + \cos q_y)$ for a square lattice. Then, using the auxiliary fermionic representation of a spin operator, the Heisenberg term is rewritten as

$$H_H = \sum_{k,k',q} J_q \Big(\frac{-1}{2} f^\dagger_{k+q\uparrow} f^\dagger_{k'-q\downarrow} f_{k'\downarrow} f_{k\uparrow} + \frac{\sigma\sigma'}{8} f^\dagger_{k+q\sigma} f^\dagger_{k'-q\sigma'} f_{k'\sigma'} f_{k\sigma} \Big).$$

In a heavy fermion system, it is well-known that the dominating magnetic correlation has an antiferromagnetic feature. Thus, the spin-triplet pairing channel is not favored and we will only consider the spin-singlet channel in our remaining derivation. Therefore, the effective interaction in the spin-singlet pairing channel is

$$H_H = \sum_{k,k',q} \frac{-3}{4} J_q f^\dagger_{k+q\uparrow} f^\dagger_{k'-q\downarrow} f_{k'\downarrow} f_{k\uparrow}. \tag{4}$$

On physical grounds, such a term describes that a pair of fermions with opposite spins feel a pairing interaction, $V_q = \frac{-3}{4} J_q$.

Let $q \to k - k'$ and symmetrize with momentum; now we have the following pairing interaction [37]

$$\begin{aligned} V_{k,k'} &= \frac{1}{2}(V_{k-k'} + V_{k+k'}) \\ &= \frac{-3J}{2}(\cos k_x \cos k'_x + \cos k_y \cos k'_y), \end{aligned}$$

which leads to the effective BCS pairing Hamiltonian

$$H_{pairing} = \sum_{k,k'} V_{k,k'} f^\dagger_{k\uparrow} f^\dagger_{-k\downarrow} f_{-k'\downarrow} f_{k'\uparrow}.$$

Considering the C_4 rotation symmetry of a square lattice [49], the present pairing interaction can be split into extended s-wave ($\gamma_k^s = \cos k_x + \cos k_y$) and $d_{x^2-y^2}$-wave ($\gamma_k^d = \cos k_x - \cos k_y$) pairing channels

$$\begin{aligned} V_{k,k'} &= V^s_{k,k'} + V^d_{k,k'}, \\ V^s_{k,k'} &= -\frac{3}{4} J_H \gamma^s_k \gamma^s_{k'}, \\ V^d_{k,k'} &= -\frac{3}{4} J_H \gamma^d_k \gamma^d_{k'}. \end{aligned}$$

In other words, the Heisenberg-like local antiferromagnetic exchange interaction may mediate extended s- and $d_{x^2-y^2}$-wave pairing on a square lattice.

For each pairing symmetry, we obtain its pairing Hamiltonian as

$$H_{pairing} = -\frac{3}{4} J_H \left(\sum_k \gamma_k f^\dagger_{k\uparrow} f^\dagger_{-k\downarrow} \right) \left(\sum_{k'} \gamma_{k'} f_{-k'\downarrow} f_{k'\uparrow} \right).$$

Following the spirit of classic BCS mean-field theory [2], we introduce the pairing order parameter

$$\Delta = -\frac{3}{4} \sum_k \gamma_k \langle f^\dagger_{k\uparrow} f^\dagger_{-k\downarrow} \rangle = -\frac{3}{4} \sum_k \gamma_k \langle f_{-k\downarrow} f_{k\uparrow} \rangle,$$

and the corresponding mean-field Hamiltonian

$$H_{pairing} = J_H \Delta \sum_k \gamma_k (f^\dagger_{k\uparrow} f^\dagger_{-k\downarrow} + f_{-k\downarrow} f_{k\uparrow}) + \frac{4 J_H \Delta^2}{3}. \tag{5}$$

Note that such a pairing Hamiltonian is identical to those in Refs. [30, 31, 47], where the RVB-like approach is used [34], i.e., a spin-singlet pairing order of auxiliary fermions in real-space is assumed to be

$$\Delta_{ij} = \langle f^\dagger_{i\uparrow} f^\dagger_{j\downarrow} - f^\dagger_{i\downarrow} f^\dagger_{j\uparrow} \rangle.$$

Although our method is similar to the conventional antiferromagnetic spin-fluctuation-exchange theory, it is equivalent to the RVB-pairing theory at least at the present mean-field level, which emphasizes the core role of local magnetic interactions [32]. In some sense, the mean-field pairing model misses the effect of the original pairing interaction; however, if the fluctuation of the pairing interaction is included, one may identify which microscopic interaction is responsible for pairing.

By adding this pairing Hamiltonian into the normal-state model Eq. (1), one obtains the desired model for heavy fermion superconductivity. In practice, the pairing between different heavy fermion quasi-particle bands is usually neglected due to the mismatch of the Fermi surface as done in Ref. [24]. Thus, the pairing Hamilto-

nian is simplified to

$$H_{pairing} = J_H\Delta\sum_k \gamma_k(\beta_k^2(A_{k\uparrow}^\dagger A_{-k\downarrow}^\dagger)+\alpha_k^2(B_{k\uparrow}^\dagger B_{-k\downarrow}^\dagger) +\alpha_k\beta_k(A_{k\uparrow}^\dagger B_{-k\downarrow}^\dagger+B_{k\uparrow}^\dagger A_{-k\downarrow}^\dagger)+\text{H.c.})+J_H\frac{4\Delta^2}{3} \simeq\sum_k[J_H\Delta_k^A(A_{k\uparrow}^\dagger A_{-k\downarrow}^\dagger+A_{-k\downarrow}A_{k\uparrow}) +J_H\Delta_k^B(B_{k\uparrow}^\dagger B_{-k\downarrow}^\dagger+B_{-k\downarrow}B_{k\uparrow})]+J_H\frac{4\Delta^2}{3}. \quad (6)$$

We have defined two gap functions, $\Delta_k^A=\Delta\gamma_k\beta_k^2$ and $\Delta_k^B=\Delta\gamma_k\alpha_k^2$, for quasi-particles A_σ and B_σ, respectively. Note that such a gap function is modified by the normal-state coherent factor, whose momentum dependence deviates from the pure pairing function, γ_k. However, the qualitative physics is unchanged by such modulation. The advantage of such a simplification is to decouple each heavy fermion quasi-particle band, which leads to two independent BCS-like mean-field Hamiltonians. Therefore, after introducing the Bogoliubov transformation for each quasi-particle band

$$A_{k\sigma}=\mu_k^A\tilde{A}_{k\sigma}-\nu_k^A\tilde{A}_{-k-\sigma}^\dagger, \quad B_{k\sigma}=\mu_k^A\tilde{B}_{k\sigma}-\nu_k^A\tilde{B}_{-k-\sigma}^\dagger, \quad (7)$$

where

$$\mu_k^A=1-\nu_k^A=\frac{1}{2}\left(1+\frac{E_k^+}{E_k^A}\right), \quad \mu_k^B=1-\nu_k^B=\frac{1}{2}\left(1+\frac{E_k^-}{E_k^B}\right),$$

the resultant Hamiltonian is

$$H=\sum_k[E_k^A\tilde{A}_{k\sigma}^\dagger\tilde{A}_{k\sigma}+E_k^B\tilde{B}_{k\sigma}^\dagger\tilde{B}_{k\sigma}] +\sum_k(E_k^++E_k^--E_k^A-E_k^B)+N_sE_0', \quad (8)$$

where the energy spectrum of the superconducting quasi-particles has the following form

$$E_k^A=\sqrt{(E_k^+)^2+(J_H\Delta_k^A)^2}, \quad E_k^B=\sqrt{(E_k^-)^2+(J_H\Delta_k^B)^2}.$$

The corresponding free energy and mean-field self-consistent equations are given in Appendix B.

The mean-field superconducting Hamiltonian for the Kondo–Heisenberg model has now been obtained. When the temperature is above the critical temperature, T_c, there still exists the normal-state described by Eq. (3), where the heavy fermion quasi-particle moves freely in the renormalized heavy Fermi liquid. If we cool the system below T_c, the normal heavy Fermi liquid transitions into the heavy fermion superconducting state with pairing of heavy quasi-particles. To avoid the instability of a quantum spin liquid or fractionalized Fermi liquid states [41], the ratio J_H/J_K should not be larger than a particular critical value. These critical values are summarized in Fig. 2.

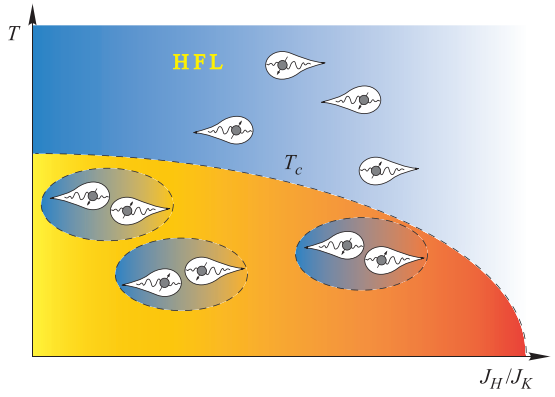

Fig. 2 Above T_c, the wandering heavy fermion quasi-particle forms a heavy fermion liquid (HFL), which undergoes a pairing instability into a heavy fermion superconductor below T_c. When J_H/J_K increases, the magnetic fluctuation is strengthened and the magnetic or spin liquid states may ultimately dominate beyond critical ratio of J_H/J_K.

4 Superfluid response formula

In this section, we will study the superfluid response function in heavy fermion superconductors. The main point of this section is to determine the superfluid response in heavy fermion superconductors; is there coupling between $\boldsymbol{A}$ and conduction electrons, auxiliary fermions, or heavy fermion quasi-particles ? As detailed in this section, we find that likely only the heavy fermion quasi-particle couples with $\boldsymbol{A}$ strongly, as depicted in Fig. 1.

4.1 Superfluid response without the auxiliary fermion

In the Kondo–Heisenberg model, by definition, $\boldsymbol{A}$ acts on a conduction electron by substitution $t_{ij}\to t_{ij}\mathrm{e}^{\mathrm{i}eA_{ij}}$, where t_{ij} is the hopping energy in real-space. Thus, the Hamiltonian is invariant under local U(1) charge gauge transformation via

$$c_\sigma\to c_\sigma\mathrm{e}^{\mathrm{i}\theta_i}, \quad A_{ij}\to A_{ij}+(\theta_i-\theta_j)/e,$$

while f_σ does not directly respond to $\boldsymbol{A}$ because it originates from the fermionic representation of spin and has no electric charge [37].

Therefore, we assume that only the conduction elec-

tron can be involved in the calculation of superfluid response.

To discuss the superfluid response function, we consider the conduction electron as being coupled to $\boldsymbol{A}_q$ via the following Hamiltonian [37]

$$\begin{aligned} H' &= \sum_{kq\sigma} e\boldsymbol{v}_k \cdot \boldsymbol{A}_q c^\dagger_{k+q\sigma} c_{k\sigma} \\ &= \sum_{kq} e\boldsymbol{v}_k \cdot \boldsymbol{A}_q (c^\dagger_{k+q\uparrow} c_{k\uparrow} + c^\dagger_{k+q\downarrow} c_{k\downarrow}) \\ &= \sum_{kq} e\boldsymbol{v}_k \cdot \boldsymbol{A}_q (c^\dagger_{k+q\uparrow} c_{k\uparrow} + c_{-k\downarrow} c^\dagger_{-k-q\downarrow}) \\ &= \sum_{kq} e\boldsymbol{v}_k \cdot \boldsymbol{A}_q \psi^\dagger_{k+q} \psi_k. \end{aligned}$$

Here, we have defined conduction electron velocity, $\boldsymbol{v}_k = \frac{\partial \varepsilon_k}{\partial k_i}$, and the Nambu spinor, $\psi^\dagger_k = (c^\dagger_{k\uparrow}, c_{-k\downarrow})$. Note that the bare vertex is simply $ie\boldsymbol{v}_k$, which leads to paramagnetic current-current correlation function

$$\begin{aligned} \Pi(q)^p_{ij} &= +e^2 \sum_k v^i_k v^j_{k+q} Tr[G(k)G(k+q)] \\ &= +e^2 \sum_k v^i_k v^j_{k+q} [G_{11}(k)G_{11}(k+q) \\ &\quad + G_{12}(k)G_{21}(k+q) + (1 \leftrightarrow 2)], \end{aligned}$$

where G is a Nambu Green's function 2×2-matrix for conduction electrons and its detailed formalism is given in Appendix A.

Inserting the explicit expression of the Green's function and setting the zero-energy limit, $i\Omega_n = 0$, and zero-momentum limit, $\boldsymbol{q} = 0$, we obtain the contribution of paramagnetic current

$$Re\Pi(q=0)^p_{ij} = +2e^2 \sum_k v^i_k v^j_k \left[\alpha^4_k \frac{\partial f_F(E^A_k)}{\partial E^A_k} + \beta^4_k \frac{\partial f_F(E^B_k)}{\partial E^B_k} \right].$$

Alternatively, the diamagnetic current is coupled to $\boldsymbol{A}$ through

$$\begin{aligned} H' &= \sum_{kq\sigma} \frac{e^2}{2m} \boldsymbol{A}^\dagger_{k'-q} \boldsymbol{A}_{k'} c^\dagger_{k+q\sigma} c_{k\sigma} \\ &= \sum_{kq} \frac{e^2}{2m} \boldsymbol{A}^\dagger_{k'-q} \cdot \boldsymbol{A}_{k'} (c^\dagger_{k+q\uparrow} c_{k\uparrow} - c_{-k-q\downarrow} c^\dagger_{-k\downarrow}) \\ &= \sum_{kq} \frac{e^2}{2m} \boldsymbol{A}^\dagger_{k'-q} \cdot \boldsymbol{A}_{k'} \psi^\dagger_{k+q} \hat{\tau}_z \psi_k. \end{aligned}$$

The effective mass tensor for a conduction electron is defined as $(\frac{1}{m})_{ij} = \frac{\partial^2 \varepsilon_k}{\partial k_i \partial k_j}$. Here, the interacting vertex is $-(\frac{e^2}{2m})_{ij} \hat{\tau}_z$ and its corresponding zero-frequency diamagnetic current-current correlation is

$$\begin{aligned} \Pi(q=0)^d_{ij} &= +e^2 \sum_k \left(\frac{1}{m}\right)_{ij} Tr[\hat{\tau}_z G(k)] \\ &= e^2 \sum_k \left(\frac{1}{m}\right)_{ij} (G_{11} - G_{22}) \\ &= e^2 \sum_k \left(\frac{-1}{m}\right)_{ij} \left(\alpha^2_k \frac{E^+_k}{E^A_k} \tanh \frac{E^A_k}{2T} \right. \\ &\quad \left. + \beta^2_k \frac{E^-_k}{E^B_k} \tanh \frac{E^B_k}{2T} \right). \end{aligned}$$

Combining the paramagnetic and diamagnetic contributions, we obtain

$$\begin{aligned} Re\Pi(q=0)_{ij} = e^2 \sum_k \left[\frac{-1}{m_{ij}} \left(\alpha^2_k \frac{E^+_k}{E^A_k} \tanh \frac{E^A_k}{2T} \right. \right. \\ \left. + \beta^2_k \frac{E^-_k}{E^B_k} \tanh \frac{E^B_k}{2T} \right) + 2v^i_k v^j_k \left(\alpha^4_k \frac{\partial f_F(E^A_k)}{\partial E^A_k} \right. \\ \left. \left. + \beta^4_k \frac{\partial f_F(E^B_k)}{\partial E^B_k} \right) \right]. \end{aligned}$$

Finally, by using of the definition of superfluid density, $\frac{\rho_{ij} e^2}{m} = Re\Pi(q=0)_{ij}$, we obtain the desirable superfluid density formula, $\rho_s \equiv \rho_{ii}$,

$$\begin{aligned} \frac{\rho_s(T)}{m} = \sum_k \left[\frac{\partial^2 \varepsilon_k}{\partial k^2_x} \left(-\alpha^2_k \frac{E^+_k}{E^A_k} \tanh \frac{E^A_k}{2T} - \beta^2_k \frac{E^-_k}{E^B_k} \tanh \frac{E^B_k}{2T} \right) \right. \\ \left. + 2 \left(\frac{\partial \varepsilon_k}{\partial k_x} \right)^2 \left(\alpha^4_k \frac{\partial f_F(E^A_k)}{\partial E^A_k} + \beta^4_k \frac{\partial f_F(E^B_k)}{\partial E^B_k} \right) \right]. \end{aligned} \tag{9}$$

Unfortunately, as shown in Fig. 3, for both $d_{x^2-y^2}$- and extended s-wave pairing symmetry, the superfluid density does not vanish at T_c, thus the formula Eq. (9) is undoubtedly invalid. The parameters we used are $t = 1$, $t' = 0.3$, $J_K = 2$, $J_H = 0.6$, and $n_c = 0.9$, which are typical values in mean-field calculations using the Kondo–Heisenberg model [30]. We will explain why this formula

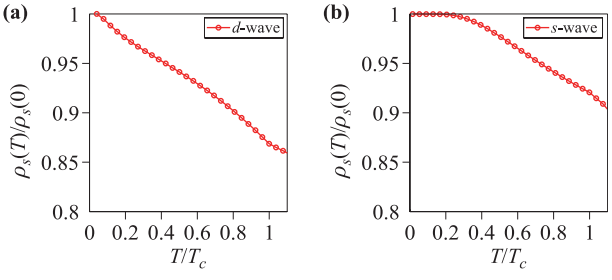

Fig. 3 Normalized superfluid density, $\rho_s(T)/\rho_s(0)$, versus normalized temperature, T/T_c, for **(a)** $d_{x^2-y^2}$- and **(b)** extended s-wave pairing symmetry by using Eq. (9).

is incorrect, although the derivation is rather straightforward.

A careful reader may note that in the normal-state mean-field Hamiltonian, Eq. (1), the conduction electron is hybridized with the auxiliary fermion via the formation of Kondo screening ($V \neq 0$ and is real). Thus repeating the argument of U(1) charge gauge transformation discussed in the beginning of this subsection, the auxiliary fermion has the transformation

$$f_{i\sigma} \to f_{i\sigma} e^{i\theta_i},$$

which means that f_σ now effectively acquires electric charge due to the well-developed Kondo hybridization in the heavy fermion liquid state. This statement is more general and beyond the present mean-field level [37]. In Appendix C, we give a brief discussion on this issue using path integral formalism.

When considering the superfluid response to an external electromagnetic field, we also need to include the contribution of the auxiliary fermion and this will be analyzed in the following subsection.

4.2 Superfluid response including the auxiliary fermion

In this section, we assume that in addition to the conduction electron, the auxiliary fermion also electromagnetically couples to $\boldsymbol{A}$. Thus, the total paramagnetic current is

$$\begin{aligned} j_i^p(q,\tau) &= j_i^c(q,\tau) + j_i^f(q,\tau), \\ j_i^c(q,\tau) &= e\sum_{k\sigma} v_c^i c_{k+q\sigma}^\dagger(\tau) c_{k\sigma}(\tau), \\ j_i^f(q,\tau) &= e\sum_{k\sigma} v_f^i f_{k+q\sigma}^\dagger(\tau) f_{k\sigma}(\tau). \end{aligned}$$

Here, $v_c^i = \partial\varepsilon_k/\partial k_i$ and $v_f^i = \partial\chi_k/\partial k_i$ are the effective velocity of the conduction electron and auxiliary fermion, respectively.

Therefore, the paramagnetic response function is

$$\begin{aligned} \Pi_{ij}(q,\tau) &= -\langle T_\tau j_i^p(q,\tau) j_i^p(-q,0)\rangle \\ &= \Pi_{ij}^{cc}(q,\tau) + \Pi_{ij}^{cf}(q,\tau) + \Pi_{ij}^{fc}(q,\tau) + \Pi_{ij}^{ff}(q,\tau). \end{aligned}$$

Note that there exist four terms, among which Π_{ij}^{cc} and Π_{ij}^{ff} denote the contribution of the conduction electron and auxiliary fermion, respectively. The remaining terms, Π_{ij}^{cc} and Π_{ij}^{ff}, are the cross-terms, which imply the quantum interference effect between different currents. In last subsection, we calculated Π_{ij}^{cc},

$$Re\Pi(q=0)_{ii}^{cc} = 2e^2\sum_k (v_c^i)^2\left[\alpha_k^4\frac{\partial f_F(E_k^A)}{\partial E_k^A} + \beta_k^4\frac{\partial f_F(E_k^B)}{\partial E_k^B}\right].$$

After a long, yet straightforward calculation, we obtain

$$Re\Pi(q=0)_{ii}^{ff} = 2e^2\sum_k (v_f^i)^2\left[\beta_k^4\frac{\partial f_F(E_k^A)}{\partial E_k^A} + \alpha_k^4\frac{\partial f_F(E_k^B)}{\partial E_k^B}\right].$$

Since $Re\Pi(q=0)_{ii}^{cf} = Re\Pi(q=0)_{ii}^{fc}$, the we calculate $\Pi(q=0)_{ii}^{cf}$,

$$\begin{aligned} \Pi(q)_{ii}^{cf} &= e^2\sum_k v_c^i v_f^i [G_{13}(k)G_{31}(k+q) \\ &\quad + G_{14}(k)G_{41}(k+q) + (1\leftrightarrow 2)]. \end{aligned}$$

After inserting the explicit form of G_{13} and G_{14}, the final result reads

$$\begin{aligned} Re\Pi(q=0)_{ii}^{cf} &= 2e^2\sum_k v_c^i v_f^i\left[\alpha_k^2\beta_k^2\frac{\partial f_F(E_k^A)}{\partial E_k^A}\right. \\ &\quad \left. + \alpha_k^2\beta_k^2\frac{\partial f_F(E_k^B)}{\partial E_k^B}\right]. \end{aligned}$$

Therefore, the paramagnetic current response is

$$\begin{aligned} Re\Pi(q=0)_{ii}^{p} &= 2e^2\sum_k\left[(\alpha_k^4(v_c^i)^2 + \beta_k^4(v_f^i)^2 + 2\alpha_k^2\beta_k^2 v_c v_f)\right. \\ &\quad \times\frac{\partial f_F(E_k^A)}{\partial E_k^A} + (\beta_k^4(v_c^i)^2 + \alpha_k^4(v_f^i)^2 \\ &\quad \left. + 2\alpha_k^2\beta_k^2 v_c v_f)\times\frac{\partial f_F(E_k^B)}{\partial E_k^B}\right] \end{aligned}$$

and the diamagnetic current response is obtained

$$\begin{aligned} &Re\Pi(q=0)_{ii}^{d} \\ &= -e^2\sum_k\left[\alpha_k^2\left(\frac{1}{m_c}\right)_{ii} + \beta_k^2\left(\frac{1}{m_f}\right)_{ii}\right]\frac{E_k^+}{E_k^A}\tanh\frac{E_k^A}{2T} \\ &\quad + \left[\beta_k^2\left(\frac{1}{m_c}\right)_{ii} + \alpha_k^2\left(\frac{1}{m_f}\right)_{ii}\right]\frac{E_k^-}{E_k^B}\tanh\frac{E_k^B}{2T}. \end{aligned}$$

Therefore, our current superfluid density formula is

$$\frac{\rho_s(T)}{m} = \frac{1}{e^2}(Re\Pi(q=0)_{ii}^d + Re\Pi(q=0)_{ii}^p). \tag{10}$$

Figure 4 shows the result of the calculation using Eq. (10), which, again, exhibits an incorrect result (using the same parameters as those in the last subsection). The reason for this may be due to the mismatch of temperature dependence between bare particles, (v_c, v_f, m_c, and

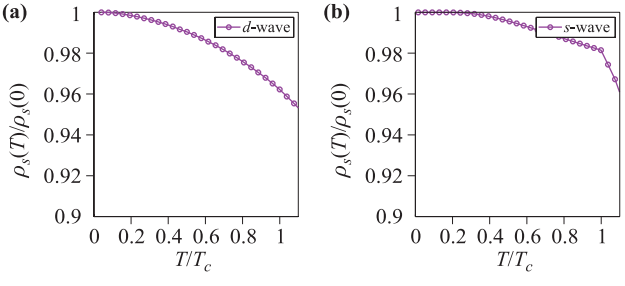

Fig. 4 Normalized superfluid density, $\rho_s(T)/\rho_s(0)$, versus normalized temperature, T/T_c, for **(a)** $d_{x^2-y^2}$- and **(b)** extended s-wave pairing symmetry using Eq. (10).

m_f), and the renormalized heavy fermion quasi-particle, E_k^A, E_k^B. In other words, the bare and renormalized particles have different temperature dependences; thus the paramagnetic contribution cannot cancel out the diamagnetic term when $T > T_c$. More generally, when calculating physical quantities at $T = 0$, since no temperature effect is involved, the underlying breakdown of the corresponding formalism is hidden. However, at finite temperatures, one may encounter the aforementioned problem.

We indeed confront a serious problem on the calculation of superfluid density.

4.3 A useful and correct superfluid response formula

In the previous section, we showed that the standard process of calculating superfluid response breaks down. However, there exists a hint to resolve this question by noting that when collective Kondo screening develops, the quasi-particles of the system are the heavy fermion quasi-particles $A_{k\sigma}$ and $B_{k\sigma}$. If all interesting physics occurs at energy-scales smaller than the width of the quasi-particle bands, E_k^+ and E_k^-, the heavy fermion quasi-particle can be seen as the only fundamental particles in our problem. Thus we may expect the low-energy thermodynamics and transport to be dominated by those heavy quasi-particles alone. In heavy fermion superconductivity, it is commonly believed that the pairing results from heavy quasi-particles and not directly involving the original conduction electron [3, 14, 37, 38]. Therefore, by considering these two factors, we propose that the heavy fermion quasi-particle is directly responsible for superfluid electromagnetic response, thus the corresponding paramagnetic current is

$$j_i^p(q,\tau)=e\sum_{k\sigma}(v_A^i A_{k+q\sigma}^\dagger(\tau)A_{k\sigma}(\tau)+v_B^i B_{k+q\sigma}^\dagger(\tau)B_{k\sigma}(\tau)),$$

where the effective velocity for heavy fermion quasi-particles A_σ and B_σ are $v_A^i = \frac{\partial E_k^+}{\partial k_i}$ and $v_B^i = \frac{\partial E_k^-}{\partial k_i}$, respectively. In addition, the diamagnetic current is found to be

$$j_i^d(q,\tau) = e^2 A_j \sum_{k\sigma}\left[\left(\frac{1}{m_A}\right)_{ij} A_{k+q\sigma}^\dagger(\tau)A_{k\sigma}(\tau) + \left(\frac{1}{m_B}\right)_{ij} B_{k+q\sigma}^\dagger(\tau)B_{k\sigma}(\tau)\right].$$

With the same treatment as in last subsection, we use these two heavy quasi-particle currents to derive Eq. (11).

$$\frac{\rho_s(T)}{m} = \sum_k\left[-\frac{\partial^2 E_k^+}{\partial k_x^2}\frac{E_k^+}{E_k^A}\tanh\frac{E_k^A}{2T} + 2\left(\frac{\partial E_k^+}{\partial k_x}\right)^2\frac{\partial f_F(E_k^A)}{\partial E_k^A} - \frac{\partial^2 E_k^-}{\partial k_x^2}\frac{E_k^-}{E_k^B}\tanh\frac{E_k^B}{2T} + 2\left(\frac{\partial E_k^-}{\partial k_x}\right)^2\frac{\partial f_F(E_k^B)}{\partial E_k^B}\right], \quad (11)$$

which is a useful and physically correct superfluid density formula and is the most important finding of the present study. As shown in Fig. 5, the superfluid density correctly vanishes when T_c is approached from the heavy fermion superconducting phase. Meanwhile, the global behavior of the temperature dependence in $\rho_s(T)$ is also consistent with general physical expectation, e.g., the extended s-wave gives rise to a flat T dependence while the nodal $d_{x^2-y^2}$-wave pairing usually leads to a power-law behavior in the low-temperature regime [2, 3].

We should emphasize that our formula, Eq. (11), is not only valid in the superconducting mean-field model, Eq. (8), but can be used in other heavy fermion superconducting models. As an example, we consider the effective model proposed in Ref. [24], which is obtained from fitting data in quasi-particle interference experiments on $CeCoIn_5$ [22, 23]. The details of their model are not given here, though we refer the reader to their original article; the calculation result is shown in Fig. 6.

When compared to the experimental data of undoped $CeCoIn_5$ in Ref. [7] (see also Fig. 6), we see that the calculated $\rho_s(T)$ does not agree with the global behavior in the experimental measurement. This may be due to the fact that the model parameters in Ref. [24] are not temperature-dependent; thus certain physical quantities, such as superfluid density, cannot be reliably calculated. Therefore, it is important to include the thermal effect and we will revisit this issue in following section.

Before ending this section, we notice that since the heavy fermion superconductors have a much longer London penetration depth, λ_L, than ordinary superconductors, e.g., about 190 nm for $CeCoIn_5$ [7], the effective mass, ($m^* = \frac{\mu_0\lambda_L^2}{\rho_s e^2} \propto \lambda_L^2$), of heavy fermion superconductors is also strongly enhanced, which implies that the

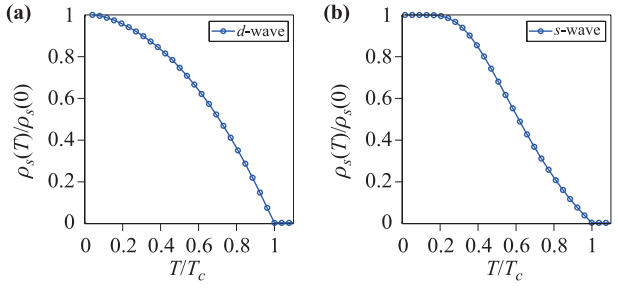

Fig. 5 Normalized superfluid density, $\rho_s(T)/\rho_s(0)$, versus normalized temperature, T/T_c, for (a) $d_{x^2-y^2}$- and (b) extended s-wave pairing symmetry using Eq. (11).

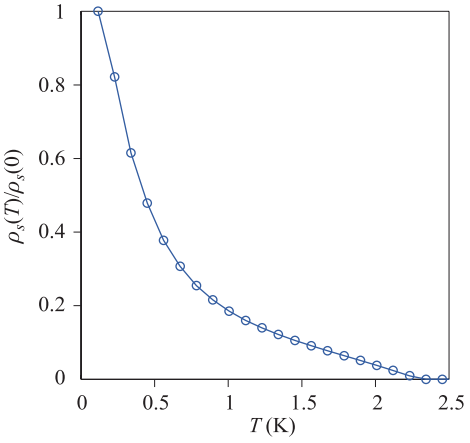

Fig. 6 Normalized superfluid density, $\rho_s(T)/\rho_s(0)$, versus temperature, T, for heavy fermion superconductor $CeCoIn_5$, using Eq. (11).

Cooper pairs in those superconductors should come from the pairing of heavy fermion quasi-particles.

5 Superfluid response in heavy fermion superconductors $CeCoIn_5$ and $Ce_{1-x}Yb_xCoIn_5$

5.1 Superfluid response in heavy fermion superconductor $CeCoIn_5$

In this section, we investigate the superfluid response in a typical heavy fermion superconductor, $CeCoIn_5$. To meet with the realistic experimental measurement, we fix model parameters as $t = -1$, $t' = 0.3$, $J_K = 2$, $J_H = 0.6$, $V = -0.2965$, $\chi = 0.2222$, and $n_c = 0.9$ [36]. The resulting normal-state Fermi surface is shown in Fig. 8, which mimics the multi-Fermi surface structure observed in ARPES measurements [50, 51].

Performing the calculation with Eq. (11) and assuming $d_{x^2-y^2}$-wave pairing, we compare our theoretical result to the experimental data in Fig. 7. From Fig. 7 we see that our theory is consistent with the global behavior of the microwave surface impedance measurements of Ref. [7] and our previous work [36]. Particularly, the observed low-temperature linear/power-law behavior of superfluid density is reproduced by our theoretical model with only the assumption of $d_{x^2-y^2}$-wave symmetry [7–11].

5.2 Issues with $Ce_{1-x}Yb_xCoIn_5$

Next, it is interesting to understand the possible pairing symmetry transition in Yb-doped $CeCoIn_5$, which is suggested by recent superfluid density measurements and inspires an exotic local electron pairing scenario [13, 26]. Effectively, Yb-doping adds an extra electron carrier into $CeCoIn_5$, thus the density of the charge carrier is modified as $n_c(x) = 0.9 + 0.8x$, where x is the nominal doping [26]. Ref. [13] finds that when $x > 0.2$, the low-temperature London penetration depth shows full gap behavior ($\Delta\lambda(T) \sim T^n$, for $n > 2$). Therefore, such anomalous behavior of the superfluid response strongly suggests that the superconducting pairing symmetry should change the structure from nodal to nodeless (see also Fig. 9).

Motivated by the above observation, authors in Ref. [26] propose that the change of pairing symmetry may result from the formation of composite pairing, i.e. electrons in two orthogonal orbits screening the same local f-electron spin to induce pairing. In this scenario, Yb-doping leads to a Lifshitz transition of a nodal Fermi surface into a fully gapped composite-pairing molecular superfluid. Thus, the nodeless behavior observed in superfluid density measurements is expected.

Here we would like to propose an alternative possibility, i.e., the change of pairing structure may simply be a doping effect and not related to the emergence of

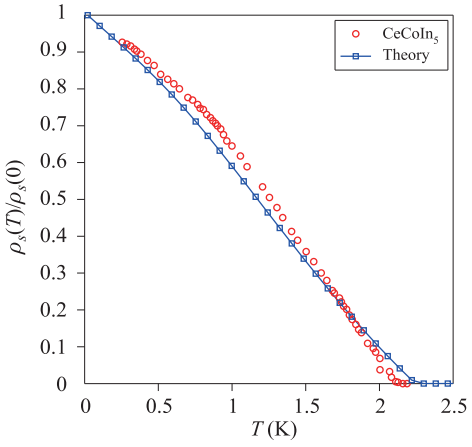

Fig. 7 Calculated normalized superfluid density (blue line and square), $\rho_s(T)/\rho_s(0)$, in the superconducting state versus temperature, T, compared to experimental data of $CeCoIn_5$ (red dot) in Ref. [7].

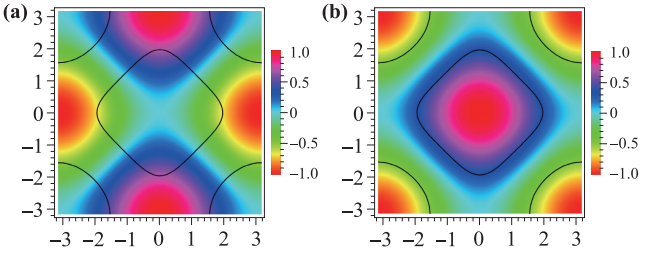

Fig. 8 Mean-field Fermi surface (bold black line), $d_{x^2-y^2}$ **(a)**, and extended s-wave **(b)** pairing function in the square lattice Brillouin zone.

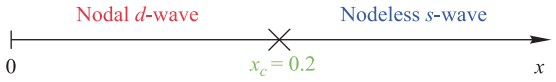

Fig. 9 Change of pairing symmetry from nodal d- to nodeless s-wave at critical Yb-doping $x_c = 0.2$ for $Ce_{1-x}Co_xIn_5$.

exotic electron pairing. To be specific, we utilize our normal-state model in Sec. 2 and calculate the doping dependence of the so-called pairing strength invented in Ref. [32],

$$\lambda^* \equiv \sum_{k\in FS} \gamma_k^2.$$

Here, the dimensionless λ^* measures the overlap of pairing function γ_k on the normal-state Fermi surface. Obviously, less (more) overlap between the nodal point/line (maximized gap zone) and Fermi surface is helpful to lower the ground-state energy and the corresponding pairing strength is larger . In other words, pairing symmetry with larger λ^* will ultimately become the true superconducting pairing instability. For the Fermi surface shown in Fig. 8, although the nodal line of $d_{x^2-y^2}$-wave has much overlap over Fermi surface, its high gap zone also has large overlap. Thus, the whole effect is to promote $d_{x^2-y^2}$-wave over the nodeless extended s-wave, which is consistent with the calculated value $\lambda_d^* = 0.957 > \lambda_s^* = 0.875$ and agrees with the observed dominated nodal d-wave feature in $CeCoIn_5$. It should be noted that the nodal line of the extended s-wave exists; however, it is not in contact with the present Fermi surface, thus, it behaves like nodeless pairing.

When considering the doping case, we plot λ^* and the effective mass ratio, m^*/m, in Fig. 10. We use $t = -1$, $t' = 0.14t$, $J_K = 1.92$, $J_H = 0.6$, $\chi = 0.2222$, and $T = 0.01$. V, μ, and λ are self-consistently solved through mean-field equations.

We find that when $n_c < 1.06$, where $n_c = 1.06$ corresponds to the observed critical doping $x_c = 0.2$, $d_{x^2-y^2}$-wave pairing dominates over extended s-wave pairing. However, if $n_c > 1.06$, the situation is inverted and the effectively nodeless extended s-wave is the dominating pairing symmetry. Therefore, this simple calculation indicates there may be a transition at $n_c = 1.06$, for $x_c = 0.2$, from nodal d-wave to nodeless s-wave symmetry. When checking the doping evolution of the effective mass, we find no clear signal of any singular behavior in either α (E_k^+) and β (E_k^-) heavy quasi-particle bands. Thus we expect the changes of electronic band or Lifshitz transition observed in ARPES and dHvA measurements may not be an active factor for the pairing symmetry transition, which is an issue in itself and needs further investigation [52, 53].

Furthermore, Fig. 11 shows the temperature-dependent superfluid density in both nodal d-wave and nodeless s-wave states for $n_c = 1.0$, where $x = 0.125 < x_c = 0.2$, and $n_c = 1.10$, where $x = 0.25 > x_c = 0.2$, respectively.

Importantly, the behaviors of the calculated results are consistent with the experimental data in Ref. [13], where the low-temperature behavior of the London penetration depth is changed from power-law to exponential when doping surpasses $x_c = 0.2$. In addition, it is noted that the pairing symmetry transition here is likely a first-order transition since the corresponding derivative of the ground-state energy is discontinuous at the putative transition point, $x = 0.2$. Thus, no radical change of an observable, such as T_c, is expected around this transition, which is also consistent with the doping evolution of Yb in Ref. [13].

Before ending this section, it is interesting to note that for the heavy fermion superconductor $CeRhIn_5$ [54], where the coexistence of antiferromagnetism and superconductivity is firmly established [55], the present superfluid response formula may also be applicable if we use a four-quasi-particle energy-band model resulting from magnetic and pairing orders. Thus, we should sum the contributions from all four bands with corresponding quasi-particle effective mass and velocity. An appropriate test for our theory will be to fit to the future London penetration depth measurement of this compound.

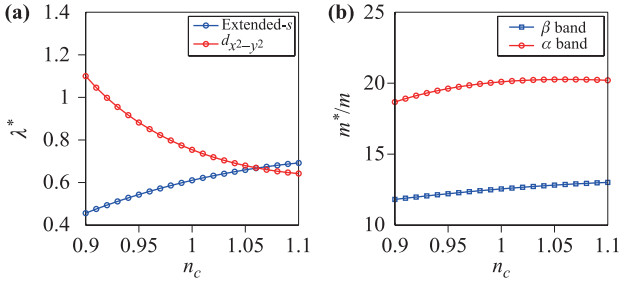

Fig. 10 Doping evolution of **(a)** pairing strength, λ^*, and **(b)** effective mass ratio, m^*/m.

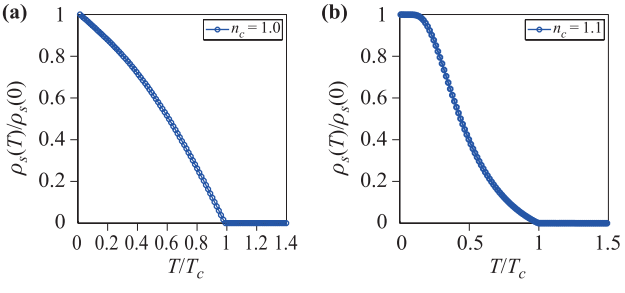

Fig. 11 The superfluid density of **(a)** nodal d-waves and **(b)** nodeless s-waves for $n_c = 1.0$ ($x = 0.125 < x_c = 0.2$) and $n_c = 1.10$ ($x = 0.25 > x_c = 0.2$), respectively.

6 Nonmagnetic impurity and non-local effects on the superfluid response

6.1 The nonmagnetic impurity effect

For realistic materials, nonmagnetic impurity scattering is ubiquitous and unavoidable. Particularly, it plays a key role in the low-temperature regime where linear-T dependence of nodal d-wave is replaced with the T^2 law [56]. Here, we give the corresponding formalism, which may be relevant to explaining realistic experimental data.

The main attribute of nonmagnetic impurity scattering is that it introduces effective damping rates, Γ_A and Γ_B, for the paired heavy quasi-particles. Then, the corresponding retarded heavy quasi-particle Green's function in the superconducting state is

$$G^R_{AA}(k,\omega)=\begin{pmatrix} G^{AA}_{11} & G^{AA}_{12} \\ G^{AA}_{21} & G^{AA}_{22}\end{pmatrix},$$

where

$$\begin{aligned} G^{AA}_{11}&=\frac{(\mu^A_k)^2}{\omega-E^A_k+\mathrm{i}\Gamma_A}+\frac{(\nu^A_k)^2}{\omega+E^A_k+\mathrm{i}\Gamma_A}\\ G^{AA}_{12}&=G^{AA}_{21}\\ &=\mu^A_k\nu^A_k\left(\frac{1}{\omega-E^A_k+\mathrm{i}\Gamma_A}-\frac{1}{\omega+E^A_k+\mathrm{i}\Gamma_A}\right)\\ G^{AA}_{22}&=\frac{(\nu^A_k)^2}{\omega-E^A_k+\mathrm{i}\Gamma_A}+\frac{(\mu^A_k)^2}{\omega+E^A_k+\mathrm{i}\Gamma_A}\end{aligned}$$

and the case for $G^R_{BB}(k,\omega)$ is similar. Next, following the same treatment as above, we obtain the expression of superfluid density

$$\begin{aligned}\frac{\rho_s(T)}{m}=\sum_k\Bigg[&\frac{\partial^2E^+_k}{\partial k_x^2}\frac{E^+_k}{E^A_k}W^A_k+2\left(\frac{\partial E^+_k}{\partial k_x}\right)^2Z^A_k\\&+\frac{\partial^2E^-_k}{\partial k_x^2}\frac{E^-_k}{E^B_k}W^B_k+2\left(\frac{\partial E^-_k}{\partial k_x}\right)^2Z^B_k\Bigg].\end{aligned}$$

Where

$$\begin{aligned}W^A_k&=\int_{-\infty}^{\infty}\mathrm{d}\omega f_F(\omega)\left[\frac{\Gamma_A/\pi}{(\omega-E^A_k)^2+\Gamma_A^2}-\frac{\Gamma_A/\pi}{(\omega+E^A_k)^2+\Gamma_A^2}\right]\\ W^B_k&=\int_{-\infty}^{\infty}\mathrm{d}\omega f_F(\omega)\left[\frac{\Gamma_B/\pi}{(\omega-E^B_k)^2+\Gamma_B^2}-\frac{\Gamma_B/\pi}{(\omega+E^B_k)^2+\Gamma_B^2}\right]\\ Z^A_k&=-\frac{1}{\pi}\int_{-\infty}^{\infty}\mathrm{d}\omega f_F(\omega)Im\frac{(\omega+\mathrm{i}\Gamma_A)^2+(E^A_k)^2}{[(\omega+\mathrm{i}\Gamma_A)^2-(E^A_k)^2]^2}\\ Z^B_k&=-\frac{1}{\pi}\int_{-\infty}^{\infty}\mathrm{d}\omega f_F(\omega)Im\frac{(\omega+\mathrm{i}\Gamma_B)^2+(E^B_k)^2}{[(\omega+\mathrm{i}\Gamma_B)^2-(E^B_k)^2]^2}.\end{aligned}$$

By using the above equations, one can inspect the explicit behavior of superfluid density in an all-temperature regime. Here, we investigate the low-temperature behavior by expanding $Z^{\alpha=A,B}_k$ [2] (W^α_k is approximated to be constant in this case)

$$Z^\alpha_k=-\frac{1}{\pi}\left[\frac{\Gamma_\alpha}{\Gamma_\alpha^2+(E^\alpha_k)^2}-\frac{\Gamma_\alpha(\Gamma_\alpha^2-3(E^\alpha_k)^2)T^2}{3(\Gamma_\alpha^2+(E^\alpha_k)^2)^3}+O(T^4)\right],$$

where the first term denotes a correction to zero-temperature superfluid density and the second term introduces the impurity-dominated T^2 dependence since this term vanishes as $\Gamma_\alpha\to 0$.

Then, for nodal superconductors, such as $d_{x^2-y^2}$-wave in undoped $CeCoIn_5$, it is found that the low-temperature superfluid density behaves as

$$\begin{aligned}\rho_s(T)\simeq&\rho_A(0)\left(1-\frac{2\Gamma_A}{\pi\Delta_A}\ln\frac{2\Delta_A}{\Gamma_A}-\frac{T^2}{3\pi\Gamma_A\Delta_A}\right),\\&+\rho_B(0)\left(1-\frac{2\Gamma_B}{\pi\Delta_B}\ln\frac{2\Delta_B}{\Gamma_B}-\frac{T^2}{3\pi\Gamma_B\Delta_B}\right),\end{aligned}$$

which is in contrast to the linear-T behavior of the pure sample. Here, $\rho_\alpha(0)$ and Δ_α are the zero-temperature superfluid density and effective gap for each quasi-particle band. We should emphasize that both the pure and impure nodal d-waves are at least qualitatively consistent with the observed power-law behaviors in $CeCoIn_5$. For La- and Nd-substituted $CeCoIn_5$ [13], this impurity induces a T^2 dirty d-wave behavior as observed by using a tunnel-diode resonator technique. Furthermore, for the possible nodeless pairing state in Yb-doped $Ce_{1-x}Yb_xCoIn_5$, no qualitative behaviors are changed by nonmagnetic impurity scattering since all low-energy excitations are fully gapped.

6.2 The non-local effect

In nodal pairing states, such as the studied $d_{x^2-y^2}$-wave, when approaching gap nodal points, its coherence length, $\xi\sim v_F/\Delta$, is larger than its λ_L. Thus, the so-called non-local effects are important [57], as they may be responsible for the observed power-law behavior of London penetration depth in $CeCoIn_5$ [7, 9, 10].

Following Ref. [57], we find that, for a specular boundary, the temperature-dependent London penetration depth is

$$\lambda(T)=\frac{2}{\pi}\int_0^\infty\frac{\mathrm{d}q}{q^2+Re\Pi(q,\omega=0)},$$

where the momentum-dependent superfluid response function is

$$\begin{aligned}&Re\Pi(q,\omega=0)\\&=-e^2\sum_k\Bigg[\frac{\partial^2E^+_k}{\partial k_x^2}\frac{E^+_k}{E^A_k}\tanh\frac{E^A_k}{2T}\\&\quad+(\mu^A_k\mu^A_{k+q}+\nu^A_k\nu^A_{k+q})^2\frac{\tanh\frac{\beta E^A_k}{2}-\tanh\frac{\beta E^A_{k+q}}{2}}{E^A_k-E^A_{k+q}}\end{aligned}$$

$$+(\mu_k^A\nu_{k+q}^A-\nu_k^A\mu_{k+q}^A)^2\frac{\tanh\frac{\beta E_k^A}{2}+\tanh\frac{\beta E_{k+q}^A}{2}}{E_k^A+E_{k+q}^A}$$
$$+\frac{\partial^2 E_k^-}{\partial k_x^2}\frac{E_k^-}{E_k^B}\tanh\frac{E_k^B}{2T}$$
$$+(\mu_k^B\mu_{k+q}^B+\nu_k^B\nu_{k+q}^B)^2\frac{\tanh\frac{\beta E_k^B}{2}-\tanh\frac{\beta E_{k+q}^B}{2}}{E_k^B-E_{k+q}^B}$$
$$+(\mu_k^B\nu_{k+q}^B-\nu_k^B\mu_{k+q}^B)^2\frac{\tanh\frac{\beta E_k^B}{2}+\tanh\frac{\beta E_{k+q}^B}{2}}{E_k^B+E_{k+q}^B}\Bigg].$$

At low temperatures ($T<T^*\sim\xi/\lambda(0)\Delta$), for nodal superconducting states, the above equation gives $\triangle\lambda(T)\equiv\lambda(T)-\lambda(0)\sim T^2$, which is similar to the nonmagnetic impurity effect and modifies the linear-T behavior. We note that Ref. [9] argued that the penetration depth of $CeCoIn_5$ is governed by this non-local electrodynamic effect rather than the nonmagnetic impurity effect.

7 Discussion and conclusion

In this work, we have systematically studied the superfluid density response formula in a pure sample and one with a nonmagnetic impurity. These formulas have been successfully applied to undoped heavy fermion superconductor, $CeCoIn_5$ and its Yb-doped counterpart, $Ce_{1-x}Yb_xCoIn_5$. Theory and experiment of those typical heavy fermion superconductors are in good agreement, which confirms our basic formalism and emphasizes the core role of heavy fermion quasi-particles. The present work may provide a useful formalism to understand and explain existing and future superfluid density experiments in heavy fermion superconductivity.

We have noted that the measurement of thermal conductivity suggests there is no pairing symmetry transition in $Ce_{1-x}Yb_xCoIn_5$, which is in contrast to the result of London penetration depth experiments. Frankly, we are still unable to judge which experiment gives the true physical behavior; however, if we use the model in Ref. [24] with our superfluid density formula, we find only a nodal d-wave state is possible.

It is intriguing to note the possibility that if the critical quasi-particle picture is still valid in heavy fermion superconducting states in proximity to the quantum critical point [58]; the paramagnetic current should contribute an extra $T^{1/2}$ due to the critical enhancement of the effective velocity. Based on our superfluid response formula, the nodal d-wave states may have $T^{3/2}$ behavior, which agrees well with existing data [7, 9, 10].

In addition, as suggested in Refs. [26, 28], since both interstitial and onsite two-channel effects are likely important for heavy fermion superconductivity, the composite pairing has to be considered seriously, which is an interesting and crucial issue for future study.

Acknowledgements Y. Zhong thank stimulating discussion with Jianhui Dai and Piers Coleman, who brings us the issue of non-local effect and composite pairing in heavy fermion superconductors. The work was supported partly by NSFC, PCSIRT (Grant No. IRT1251), the Fundamental Research Funds for the Central Universities and the national program for basic research of China.

Contribution statement Y. Zhong suggested the project and carried out the calculation. All of authors wrote and revised this article.

Appendix A Single particle Green's function

In the superconducting state, the single particle imaginary time Green's function is defined as follows

$$G(k,\tau)\equiv-\langle T_\tau(c_{k\uparrow}(\tau),c_{-k\downarrow}^\dagger(\tau),f_{k\uparrow}(\tau),f_{-k\downarrow}^\dagger(\tau))\otimes\begin{pmatrix}c_{k\uparrow}^\dagger\\c_{-k\downarrow}\\f_{k\uparrow}^\dagger\\f_{-k\downarrow}\end{pmatrix}\rangle=\begin{pmatrix}G_{11}&G_{12}&G_{13}&G_{14}\\G_{21}&G_{22}&G_{23}&G_{24}\\G_{31}&G_{32}&G_{33}&G_{34}\\G_{41}&G_{42}&G_{43}&G_{44}\end{pmatrix}.$$

In the superconducting mean-field Hamiltonian, the matrix element in momentum-energy representation reads

$$G_{11}(k)=\alpha_k^2\left[\frac{(\mu_k^A)^2}{\mathrm{i}\omega_n-E_k^A}+\frac{(\nu_k^A)^2}{\mathrm{i}\omega_n+E_k^A}\right]+\beta_k^2\left[\frac{(\mu_k^B)^2}{\mathrm{i}\omega_n-E_k^B}+\frac{(\nu_k^B)^2}{\mathrm{i}\omega_n+E_k^B}\right]$$
$$G_{12}(k)=G_{21}(k)=\alpha_k^2\mu_k^A\nu_k^A\left(\frac{1}{\mathrm{i}\omega_n-E_k^A}-\frac{1}{\mathrm{i}\omega_n+E_k^A}\right)+\beta_k^2\mu_k^B\nu_k^B\left(\frac{1}{\mathrm{i}\omega_n-E_k^B}-\frac{1}{\mathrm{i}\omega_n+E_k^B}\right)$$
$$G_{22}(k)=\alpha_k^2\left[\frac{(\nu_k^A)^2}{\mathrm{i}\omega_n-E_k^A}+\frac{(\mu_k^A)^2}{\mathrm{i}\omega_n+E_k^A}\right]+\beta_k^2\left[\frac{(\nu_k^B)^2}{\mathrm{i}\omega_n-E_k^B}+\frac{(\mu_k^B)^2}{\mathrm{i}\omega_n+E_k^B}\right]$$
$$G_{13}(k)=G_{31}(k)=\alpha_k\beta_k\left[\frac{(\mu_k^A)^2}{\mathrm{i}\omega_n-E_k^A}+\frac{(\nu_k^A)^2}{\mathrm{i}\omega_n+E_k^A}\right]-\alpha_k\beta_k\left[\frac{(\mu_k^B)^2}{\mathrm{i}\omega_n-E_k^B}+\frac{(\nu_k^B)^2}{\mathrm{i}\omega_n+E_k^B}\right]$$

$$
\begin{aligned}
G_{14}(k) &= G_{41}(k) = G_{23}(k) = G_{32}(k) \\
&= \alpha_k\beta_k\mu_k^A\nu_k^A\left(\frac{1}{\mathrm{i}\omega_n - E_k^A} - \frac{1}{\mathrm{i}\omega_n + E_k^A}\right) \\
&\quad -\alpha_k\beta_k\mu_k^B\nu_k^B\left(\frac{1}{\mathrm{i}\omega_n - E_k^B} - \frac{1}{\mathrm{i}\omega_n + E_k^B}\right) \\
G_{24}(k) &= G_{42}(k) = \alpha_k\beta_k\left[\frac{(\nu_k^A)^2}{\mathrm{i}\omega_n - E_k^A} + \frac{(\mu_k^A)^2}{\mathrm{i}\omega_n + E_k^A}\right] \\
&\quad -\alpha_k\beta_k\left[\frac{(\nu_k^B)^2}{\mathrm{i}\omega_n - E_k^B} + \frac{(\mu_k^B)^2}{\mathrm{i}\omega_n + E_k^B}\right]. \\
G_{33}(k) &= \beta_k^2\left[\frac{(\mu_k^A)^2}{\mathrm{i}\omega_n - E_k^A} + \frac{(\nu_k^A)^2}{\mathrm{i}\omega_n + E_k^A}\right] \\
&\quad +\alpha_k^2\left[\frac{(\mu_k^B)^2}{\mathrm{i}\omega_n - E_k^B} + \frac{(\nu_k^B)^2}{\mathrm{i}\omega_n + E_k^B}\right] \\
G_{34}(k) &= G_{43}(k) = \beta_k^2\mu_k^A\nu_k^A\left(\frac{1}{\mathrm{i}\omega_n - E_k^A} - \frac{1}{\mathrm{i}\omega_n + E_k^A}\right) \\
&\quad +\alpha_k^2\mu_k^B\nu_k^B\left(\frac{1}{\mathrm{i}\omega_n - E_k^B} - \frac{1}{\mathrm{i}\omega_n + E_k^B}\right) \\
G_{44}(k) &= \beta_k^2\left[\frac{(\nu_k^A)^2}{\mathrm{i}\omega_n - E_k^A} + \frac{(\mu_k^A)^2}{\mathrm{i}\omega_n + E_k^A}\right] \\
&\quad +\alpha_k^2\left[\frac{(\nu_k^B)^2}{\mathrm{i}\omega_n - E_k^B} + \frac{(\mu_k^B)^2}{\mathrm{i}\omega_n + E_k^B}\right].
\end{aligned}
$$

Appendix B Free energy and mean-field equation in the heavy fermion superconducting state

Using the diagnolized mean-field Hamiltonian in Eq. (8), we readily obtain the free energy

$$
\begin{aligned}
F &= -2T\sum_k[\ln(1+\mathrm{e}^{-\beta E_k^A}) + \ln(1+\mathrm{e}^{-\beta E_k^B})] \\
&\quad +\sum_k(\varepsilon_k + \chi_k - E_k^A - E_k^B) + N_s E_0'
\end{aligned}
$$

Then, by minimizing the free energy function versus mean-field parameters V, χ, λ, μ, and Δ, we obtain the following five self-consistent equations:

$$
\begin{aligned}
2 &= J_K\sum_k\frac{1}{E_{0k}}\left(\frac{E_k^+}{E_k^A}\tanh\frac{\beta E_k^A}{2} - \frac{E_k^-}{E_k^B}\tanh\frac{\beta E_k^B}{2}\right) \\
2\chi &= J_K\sum_k\eta_k\left(\beta_k^2\frac{E_k^+}{E_k^A}\tanh\frac{\beta E_k^A}{2} + \alpha_k^2\frac{E_k^-}{E_k^B}\tanh\frac{\beta E_k^B}{2}\right) \\
0 &= \sum_k\left(2\beta_k^2\frac{E_k^+}{E_k^A}\tanh\frac{\beta E_k^A}{2} + 2\alpha_k^2\frac{E_k^-}{E_k^B}\tanh\frac{\beta E_k^B}{2}\right) \\
2(n_c-1) &= -\sum_k\left(2\alpha_k^2\frac{E_k^+}{E_k^A}\tanh\frac{\beta E_k^A}{2}\right. \\
&\quad \left.+2\beta_k^2\frac{E_k^-}{E_k^B}\tanh\frac{\beta E_k^B}{2}\right)
\end{aligned}
$$

$$
\Delta^2 = J_H\sum_k\left[\frac{(\Delta_k^A)^2}{2E_k^A}\tanh\frac{\beta E_k^A}{2} + \frac{(\Delta_k^B)^2}{2E_k^B}\tanh\frac{\beta E_k^B}{2}\right].
$$

Appendix C The charged auxiliary fermion

In this section, we follow the argument of Ref. [37] to explain the fact that auxiliary fermion has acquired electric charge via Kondo screening in the heavy fermion liquid state.

In the literature, the finite temperature or imaginary-time path integral formalism is often used and the corresponding formula is [29, 37, 41]

$$
Z = \int\mathcal{D}\bar{V}\mathcal{D}V\,D\lambda\mathcal{D}\bar{\chi}\mathcal{D}\chi\mathcal{D}c^\dagger\mathcal{D}c\mathcal{D}f^\dagger\mathcal{D}f\mathrm{e}^{-S},
$$

and the action reads

$$
\begin{aligned}
S &= \int_0^\beta\left\{\sum_{k\alpha}c_{k\alpha}^\dagger(\partial_\tau+\varepsilon_k)c_{k\alpha} + \sum_{i\alpha}f_{i\alpha}^\dagger(\partial_\tau+\mathrm{i}\lambda_i)f_{i\alpha}\right. \\
&\quad +\frac{J_K}{2}\sum_{i\alpha}[\bar{V}_i(c_{i\alpha}^\dagger f_{i\alpha}) + V_i(f_{i\alpha}^\dagger c_{i\alpha})] \\
&\quad +\frac{J_H}{2}\sum_{\langle ij\rangle\alpha}[\bar{\chi}_{ij}(f_{i\alpha}^\dagger f_{j\alpha}) + \chi_{ij}(f_{j\alpha}^\dagger f_{i\alpha})] \\
&\quad \left.+N\left(J_K\sum_i\frac{|V_i|^2}{4} + J_H\sum_{\langle ij\rangle}\frac{|\chi_{ij}|^2}{4} - \mathrm{i}\sum_i\lambda_i q\right)\right\}.
\end{aligned}
$$

Here, $q = 1/N$ and $N = 2$ for the physical spin case and all mean-field order parameters are now dynamic fields. Evidently, the dynamic Lagrangian parameter, λ, enforces the constraint if we integrate it out. Meanwhile, integrating out the valence-bond order, χ_{ij}, will recover the original Heisenberg interaction term. Thus, the above path integral formalism is an exact description of the original Kondo–Heisenberg model [37, 41].

Then, we set $V_i = V_i\mathrm{e}^{\mathrm{i}\phi_i}$ where the new V_i is a real field and absorbs the phase part into f_i. This gives a substitute $\lambda_i \to \lambda_i + \partial_\tau\phi_i$ and the Kondo hybridizing field V_i is real.

$$
\begin{aligned}
S &= \int_0^\beta\left\{\sum_{k\alpha}c_{k\alpha}^\dagger(\partial_\tau+\varepsilon_k)c_{k\alpha}\right. \\
&\quad +\sum_{i\alpha}f_{i\alpha}^\dagger[\partial_\tau+\mathrm{i}(\lambda_i+\partial_\tau\phi_i)]f_{i\alpha} \\
&\quad +\frac{J_K}{2}\sum_{i\alpha}V_i(c_{i\alpha}^\dagger f_{i\alpha} + f_{i\alpha}^\dagger c_{i\alpha}) \\
&\quad +\frac{J_H}{2}\sum_{\langle ij\rangle\alpha}[\bar{\chi}_{ij}(f_{i\alpha}^\dagger f_{j\alpha}) + \chi_{ij}(f_{j\alpha}^\dagger f_{i\alpha})] \\
&\quad \left.+N\left(J_K\sum_i\frac{V_i^2}{4} + J_H\sum_{\langle ij\rangle}\frac{|\chi_{ij}|^2}{4} - \mathrm{i}\sum_i\lambda_i q\right)\right\}.
\end{aligned}
$$

As emphasized in Ref. [37], when the Kondo screening is developed, the internal gauge symmetry is lost in the above action due to the Anderson–Higgs mechanism, which states that the absorption of the gapless phase into gauge field leads to the mass of the gauge field itself. In other words, the f-fermion appears to be physical object and is free of internal gauge structure.

Furthermore, we can define a new λ_i to absorb $\partial_\tau \phi_i$,

$$\begin{aligned} S = \int_0^\beta \Bigg\{ & \sum_{k\alpha} c^\dagger_{k\alpha}(\partial_\tau + \varepsilon_k) c_{k\alpha} + \sum_{i\alpha} f^\dagger_{i\alpha}(\partial_\tau + \mathrm{i}\lambda_i) f_{i\alpha} \\ & + \frac{J_K}{2} \sum_{i\alpha} V_i (c^\dagger_{i\alpha} f_{i\alpha} + f^\dagger_{i\alpha} c_{i\alpha}) \\ & + \frac{J_H}{2} \sum_{\langle ij\rangle \alpha} [\bar{\chi}_{ij}(f^\dagger_{i\alpha} f_{j\alpha}) + \chi_{ij}(f^\dagger_{j\alpha} f_{i\alpha})] \\ & + N\left(J_K \sum_i \frac{V_i^2}{4} + J_H \sum_{\langle ij\rangle} \frac{|\chi_{ij}|^2}{4} - \mathrm{i} \sum_i \lambda_i q \right) \Bigg\}. \end{aligned}$$

Here, we should note the integral measurement of λ_i is changed from $\{-\infty, \infty\}$ to the complex plane; thus, the number of degrees of freedom is unchanged.

$$\int_{-\infty}^{\infty} \frac{\mathrm{d}\lambda_i}{2\pi} [\ldots] \to \int_c \frac{\mathrm{d}\lambda_i}{2\pi} [\ldots].$$

Now, under the electrodynamic gauge transformation, $c_{i\alpha} \to c_{i\alpha} e^{i\theta_i}$, we have to use $f_{i\alpha} \to f_{i\alpha} e^{i\theta_i}$ since V_i is real and chargeless. This clearly promotes the physical charge into the composite f-fermion and it can respond to the external electromagnetic field as a true physical electron excitation [37]. Furthermore, the full action including external electromagnetic field is given by

$$\begin{aligned} S = \int_0^\beta \Bigg\{ & \sum_{ij\alpha} c^\dagger_{i\alpha}(\partial_\tau \delta_{ij} + t_{ij} \mathrm{e}^{\mathrm{i}eA_{ij}}) c_{j\alpha} \\ & + \sum_{i\alpha} f^\dagger_{i\alpha}(\partial_\tau + \mathrm{i}\lambda_i) f_{i\alpha} + \frac{J_K}{2} \sum_{i\alpha} V_i [c^\dagger_{i\alpha} f_{i\alpha} + f^\dagger_{i\alpha} c_{i\alpha}] \\ & + \frac{J_H}{2} \sum_{\langle ij\rangle \alpha} [\bar{\chi}_{ij} \mathrm{e}^{-\mathrm{i}eA_{ij}} (f^\dagger_{i\alpha} f_{j\alpha}) + \chi_{ij} \mathrm{e}^{\mathrm{i}eA_{ij}} (f^\dagger_{j\alpha} f_{i\alpha})] \\ & + N\left(J_K \sum_i \frac{V_i^2}{4} + J_H \sum_{\langle ij\rangle} \frac{|\chi_{ij}|^2}{4} - \mathrm{i} \sum_i \lambda_i q \right) \Bigg\}, \end{aligned}$$

where both conduction electrons and auxiliary fermions are coupled to external electromagnetic field.

References

1. M. Tinkham, Introduction to Superconductivity, New York: McGraw-Hill, 1996
2. T. Xiang, d-wave superconductor, Beijing: Science Publisher, 2007 (in Chinese)
3. C. P. Poole, R. Prozorov, H. A. Farach, and R. J. Creswick, Superconductivity, 3rd Ed., Amsterdam: Elsevier, 2014
4. W. N. Hardy, D. A. Bonn, D. C. Morgan, R. Liang, and K. Zhang, Precision measurements of the temperature dependence of l in $YBa_2Cu_3O_{6.95}$: Strong evidence for nodes in the gap function, *Phys. Rev. Lett.* 70(25), 3999 (1993)
5. M. S. Kim, J. A. Skinta, T. R. Lemberger, A. Tsukada, and M. Naito, Magnetic penetration depth measurements of $Pr_{2-x}Ce_xCuO_{4-d}$ films on Buffered substrates: Evidence for a nodeless gap, *Phys. Rev. Lett.* 91(8), 087001 (2003)
6. R. Prozorov and V. G. Kogan, London penetration depth in iron-based superconductors, *Rep. Prog. Phys.* 74(12), 124505 (2011)
7. R. J. Ormeno, A. Sibley, C. E. Gough, S. Sebastian, and I. R. Fisher, Microwave conductivity and penetration depth in the heavy fermion superconductor $CeCoIn_5$, *Phys. Rev. Lett.* 88(4), 047005 (2002)
8. S. Özcan, D. M. Broun, B. Morgan, R. K. W. Haselwimmer, J. L. Sarrao, S. Kamal, C. P. Bidinosti, P. J. Turner, M. Raudsepp, and J. R. Waldram, London penetration depth measurements of the heavy-fermion superconductor $CeCoIn_5$ near a magnetic quantum critical point, *Europhys. Lett.* 62(3), 412 (2003)
9. E. E. M. Chia, D. J. Van Harlingen, M. B. Salamon, B. D. Yanoff, I. Bonalde, and J. L. Sarrao, Nonlocality and strong coupling in the heavy fermion superconductor $CeCoIn_5$: A penetration depth study, *Phys. Rev. B* 67(1), 014527 (2003)
10. K. Hashimoto, Y. Mizukami, R. Katsumata, H. Shishido, M. Yamashita, H. Ikeda, Y. Matsuda, J. A. Schlueter, J. D. Fletcher, A. Carrington, D. Gnida, D. Kaczorowski, and T. Shibauchi, Anomalous superfluid density in quantum critical superconductors, *Proc. Natl. Acad. Sci. USA* 110(9), 3293 (2013)
11. C. J. S. Truncik, W. A. Huttema, P. J. Turner, S. Özcan, N. C. Murphy, P. R. Carrière, E. Thewalt, K. J. Morse, A. J. Koenig, J. L. Sarrao, and D. M. Broun, Nodal quasiparticle dynamics in the heavy fermion superconductor $CeCoIn_5$ revealed by precision microwave spectroscopy, *Nat. Commun.* 4, 2477 (2013)
12. L. Shu, D. E. MacLaughlin, C. M. Varma, O. O. Bernal, P. C. Ho, R. H. Fukuda, X. P. Shen, and M. B. Maple, Landau renormalizations of superfluid density in the heavy-fermion superconductor $CeCoIn_5$, *Phys. Rev. Lett.* 113(16), 166401 (2014)
13. H. Kim, M. A. Tanatar, R. Flint, C. Petrovic, R. Hu, B. D. White, I. K. Lum, M. B. Maple, and R. Prozorov, Nodal to nodeless superconducting energy-gap structure change concomitant with Fermi-surface reconstruction in the heavy-fermion compound $CeCoIn_5$, *Phys. Rev. Lett.* 114(2), 027003 (2015)

14. C. Petrovic, P. G. Pagliuso, M. F. Hundley, R. Movshovich, J. L. Sarrao, J. D. Thompson, Z. Fisk, and P. Monthoux, Heavy-fermion superconductivity in $CeCoIn_5$ at 2.3 K, *J. Phys.: Condens. Matter* 13(17), 337 (2001)

15. R. Movshovich, M. Jaime, J. D. Thompson, C. Petrovic, Z. Fisk, P. G. Pagliuso, and J. L. Sarrao, Unconventional superconductivity in $CeIrIn_5$ and $CeCoIn_5$: Specific heat and thermal conductivity studies, *Phys. Rev. Lett.* 86(22), 5152 (2001)

16. K. An, T. Sakakibara, R. Settai, Y. Onuki, M. Hiragi, M. Ichioka, and K. Machida, Sign reversal of field-angle resolved heat capacity oscillations in a heavy fermion superconductor $CeCoIn_5$ and d_{x2-y2} pairing symmetry, *Phys. Rev. Lett.* 104(3), 037002 (2010)

17. K. Izawa, H. Yamaguchi, Y. Matsuda, H. Shishido, R. Settai, and Y. Onuki, Angular position of nodes in the superconducting gap of quasi-2D heavy-fermion superconductor $CeCoIn_5$, *Phys. Rev. Lett.* 87(5), 057002 (2001)

18. T. Tayama, A. Harita, T. Sakakibara, Y. Haga, H. Shishido, R. Settai and Y. Onuki, Unconventional heavy-fermion superconductor $CeCoIn_5$: dc magnetization study at temperatures down to 50 mK, *Phys. Rev. B* **65**, 180504(R) (2002)

19. Y. Kohori, Y. Yamato, Y. Iwamoto, T. Kohara, E. D. Bauer, M. B. Maple, and J. L. Sarrao, NMR and NQR studies of the heavy fermion superconductors $CeTIn_5$ (T=Co and Ir), *Phys. Rev. B* 64(13), 134526 (2001)

20. S. Ernst, S. Wirth, F. Steglich, Z. Fisk, J. L. Sarrao, and J. D. Thompson, Scanning tunneling microscopy studies on $CeCoIn_5$ and $CeIrIn_5$, *Phys. Status Solidi B* 247(3), 624 (2010)

21. C. Stock, C. Broholm, J. Hudis, H. J. Kang, and C. Petrovic, Spin resonance in the d-wave superconductor $CeCoIn_5$, *Phys. Rev. Lett.* 100(8), 087001 (2008)

22. M. P. Allan, F. Massee, D. K. Morr, J. Van Dyke, A. W. Rost, A. P. Mackenzie, C. Petrovic, and J. C. Davis, Imaging Cooper pairing of heavy fermions in $CeCoIn_5$, *Nat. Phys.* 9(8), 468 (2013)

23. B. B. Zhou, S. Misra, E. H. da Silva Neto, P. Aynajian, R. E. Baumbach, J. D. Thompson, E. D. Bauer, and A. Yazdani, Visualizing nodal heavy fermion superconductivity in $CeCoIn_5$, *Nat. Phys.* 9(8), 474 (2013)

24. J. Van Dyke, F. Massee, M. P. Allan, J. C. Davis, C. Petrovic, and D. K. Morr, Direct evidence for a magnetic f-electron mediated pairing mechanism of heavy-fermion superconductivity in $CeCoIn_5$, *Proc. Natl. Acad. Sci. USA* 111(32), 11663 (2014)

25. Y. Xu, J. K. Dong, L. I. Lum, J. Zhang, X. C. Hong, L. P. He, K. F. Wang, Y. C. Ma, C. Petrovic, M. B. Maple, L. Shu, and S. Y. Li, Universal heat conduction in $Ce_{1-x}Yb_xCoIn_5$: Evidence for robust nodal d-wave superconducting gap, *Phys. Rev. B* 93(6), 064502 (2016)

26. O. Erten, R. Flint, and P. Coleman, Molecular pairing and fully gapped superconductivity in Yb-doped $CeCoIn_5$, *Phys. Rev. Lett.* 114(2), 027002 (2015)

27. C. M. Varma, K. Miyake, and S. Schmitt-Rink, London penetration depth of heavy-fermion superconductors, *Phys. Rev. Lett.* 57(5), 626 (1986)

28. P. Coleman, A. M. Tsvelik, N. Andrei, and H. Y. Kee, Co-operative Kondo effect in the two-channel Kondo lattice, *Phys. Rev. B* 60(5), 3608 (1999)

29. P. Coleman and N. Andrei, Kondo-stabilised spin liquids and heavy fermion superconductivity, *J. Phys.: Condens. Matter* 1(26), 4057 (1989)

30. Y. Liu, H. Li, G. M. Zhang, and L. Yu, d-wave superconductivity induced by short-range antiferromagnetic correlations in the two-dimensional Kondo lattice model, *Phys. Rev. B* 86(2), 024526 (2012)

31. Y. Liu, G. M. Zhang, and L. Yu, Pairing symmetry of heavy fermion superconductivity in the two-dimensional Kondo–Heisenberg lattice model, *Chin. Phys. Lett.* 31(8), 087102 (2014)

32. J. P. Hu and H. Ding, Local antiferromagnetic exchange and collaborative Fermi surface as key ingredients of high temperature superconductors, *Sci. Rep.* 2, 381 (2012)

33. D. J. Scalapino, A common thread: The pairing interaction for unconventional superconductors, *Rev. Mod. Phys.* 84(4), 1383 (2012)

34. P. W. Anderson, P. A. Lee, M. Randeria, T. M. Rice, N. Trivedi, and F. C. Zhang, The physics behind high temperature superconducting cuprates: The plain vanilla version of RVB, *J. Phys.: Condens. Matter* 16(24), R755 (2004)

35. P. A. Lee, N. Nagaosa, and X. G. Wen, Doping a Mott insulator: Physics of high-temperature superconductivity, *Rev. Mod. Phys.* 78(1), 17 (2006)

36. Y. Zhong, L. Zhang, H. T. Lu, and H. G. Luo, Fermionology in the Kondo–Heisenberg model: the case of $CeCoIn_5$, *Eur. Phys. J. B* 88(9), 238 (2015)

37. P. Coleman, Introduction to Many Body Physics, Chapters 15 to 18, Cambridge: Cambridge University Press, 2015

38. C. Pfleiderer, Superconducting phases of f-electron compounds, *Rev. Mod. Phys.* 81(4), 1551 (2009)

39. L. Shu, D. E. MacLaughlin, W. P. Beyermann, R. H. Heffner, G. D. Morris, O. O. Bernal, F. D. Callaghan, J. E. Sonier, W. M. Yuhasz, N. A. Frederick, and M. B. Maple, Penetration depth, multiband superconductivity, and absence of muon-induced perturbation in superconducting $PrOs_4Sb_{12}$, *Phys. Rev. B* 79(17), 174511 (2009)

40. X. Y. Tee, H. G. Luo, T. Xiang, D. Vandervelde, M. B. Salamon, H. Sugawara, H. Sato, C. Panagopoulos, and E. E. M. Chia, Penetration depth study of $LaOs_4Sb_{12}$: Multiband s-wave superconductivity, *Phys. Rev. B* 86(6), 064518 (2012)

41. T. Senthil, M. Vojta, and S. Sachdev, Weak magnetism and non-Fermi liquids near heavy-fermion critical points, *Phys. Rev. B* 69(3), 035111 (2004)
42. Y. Zhong, K. Liu, Y. F. Wang, Y. Q. Wang, and H. G. Luo, Half-filled Kondo lattice on the honeycomb lattice, *Eur. Phys. J. B* 86(5), 195 (2013)
43. L. Zhang, Y. F. Wang, Y. Zhong, and H. G. Luo, Extended s-wave pairing symmetry on the triangular lattice heavy fermion system, *Eur. Phys. J. B* 88(10), 267 (2015)
44. A. Ramires and P. Coleman, Supersymmetric approach to heavy fermion systems, *Phys. Rev. B* 93(3), 035120 (2016)
45. N. Read and D. Newns, On the solution of the Coqblin-Schrieffer Hamiltonian by the large-N expansion technique, *J. Phys. C* 16, 3273 (1983)
46. P. Coleman, Mixed valence as an almost broken symmetry, *Phys. Rev. B* 35(10), 5072 (1987)
47. M. Z. Asadzadeh, M. Fabrizio, and F. Becca, Superconductivity from spoiling magnetism in the Kondo lattice model, *Phys. Rev. B* 90(20), 205113 (2014)
48. P. Coleman and A. H. Nevidomskyy, Frustration and the Kondo effect in heavy fermion materials, *J. Low Temp. Phys.* 161(1–2), 182 (2010)
49. G. Kotliar and J. Liu, Superexchange mechanism and d-wave superconductivity, *Phys. Rev. B* 38(7), 5142 (1988)
50. A. Koitzsch, I. Opahle, S. Elgazzar, S. V. Borisenko, J. Geck, V. B. Zabolotnyy, D. Inosov, H. Shiozawa, M. Richter, M. Knupfer, J. Fink, B. Büchner, E. D. Bauer, J. L. Sarrao, and R. Follath, Electronic structure of $CeCoIn_5$ from angle-resolved photoemission spectroscopy, *Phys. Rev. B* 79(7), 075104 (2009)
51. X. W. Jia, Y. Liu, L. Yu, J. F. He, L. Zhao, W. T. Zhang, H. Y. Liu, G. D. Liu, S. L. He, J. Zhang, W. Lu, Y. Wu, X. L. Dong, L. L. Sun, G. L. Wang, Y. Zhu, X. Y. Wang, Q. J. Peng, Z. M. Wang, S. J. Zhang, F. Yang, Z. Y. Xu, C. T. Chen, and X. J. Zhou, Growth, characterization and fermi surface of heavy fermion $CeCoIn_5$ superconductor, *Chin. Phys. Lett.* 28(5), 057401 (2011)
52. L. Dudy, J. D. Denlinger, L. Shu, M. Janoschek, J. W. Allen, and M. B. Maple, Yb valence change in $Ce_{1-x}Yb_xCoIn_5$ from spectroscopy and bulk properties, *Phys. Rev. B* 88(16), 165118 (2013)
53. A. Polyakov, O. Ignatchik, B. Bergk, K. Götze, A. D. Bianchi, S. Blackburn, B. Prévost, G. Seyfarth, M. Côté, D. Hurt, C. Capan, Z. Fisk, R. G. Goodrich, I. Sheikin, M. Richter, and J. Wosnitza, Fermi-surface evolution in Yb-substituted $CeCoIn_5$, *Phys. Rev. B* 85(24), 245119 (2012)
54. H. Hegger, C. Petrovic, E. G. Moshopoulou, M. F. Hundley, J. L. Sarrao, Z. Fisk, and J. D. Thompson, Pressure-induced superconductivity in Quasi-2D $CeRhIn_5$, *Phys. Rev. Lett.* 84(21), 4986 (2000)
55. T. Park, F. Ronning, H.-Q. Yuan, M. B. Salamon, R. Movshovich, J. L. Sarrao, and J. D. Thompson, Hidden magnetism and quantum criticality in the heavy fermion superconductor $CeRhIn_5$, *Nature* (London) **440**, 65 (2006)
56. P. J. Hirschfeld and N. Goldenfeld, Effect of strong scattering on the low-temperature penetration depth of a d-wave superconductor, *Phys. Rev. B* 48(6), 4219 (1993)
57. I. Kosztin and A. J. Leggett, Nonlocal effects on the magnetic penetration depth in d-wave superconductors, *Phys. Rev. Lett.* 79(1), 135 (1997)
58. E. Abrahams, J. Schmalian, and P. Wölfle, Strong-coupling theory of heavy-fermion criticality, *Phys. Rev. B* 90(4), 045105 (2014)